

1

Analysis of Wind Effects on Tall Buildings of Irregular Cross-Sections Using Numerical Simulation

Arya S M, Deepak Sharma, Ritu Raj*

Department of Civil Engineering, Delhi Technological University, Delhi, India

*Corresponding author email: rituraj@dtu.ac.in

Abstract

The number of buildings built increased as the population grew, which in turn reduced the amount of available land. As a result of this more and more high-rise structures are being constructed to meet the existing demands. These high-rise structures are more vulnerable than a low-rise structure to dynamic loadings like wind load and earthquake load. The wind loads are such that, its effect increases as height increases. This study uses numerical simulations to examine the impact of wind load on high-rise structures with two alternative "Fish" shapes- Model 1 (S-1) and Model 2 (S-2). CFD simulation software ANSYS is used here. Both the shapes are analysed in isolated condition. Angles of wind incidence ranges from 0° to 180° . The scale used here is 1:100. The coefficient of pressure at different wind incidence angles and velocity streamlines of both models are found in the result part. Both the model shows almost similar variation in C_p in majority of faces under different wind incidence angles. Model 2 exhibited better streamline pattern at every angles.

Keywords

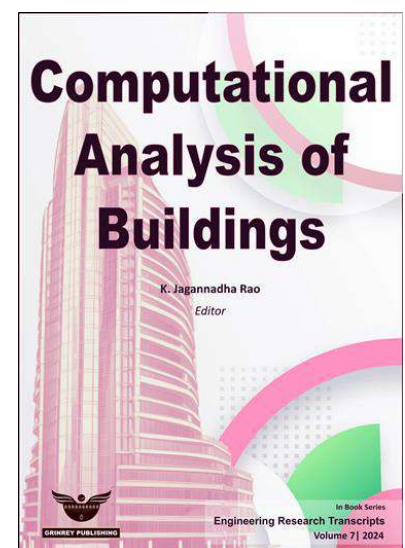
Fish shape, CFD simulation, k- ϵ turbulence model

Received: 04 Apr 2023 | Accepted: 28 Feb 2024 | Online: 08 Mar 2024

Cite this article

Arya S M, Deepak Sharma and Ritu Raj (2024). Analysis of Wind Effects on Tall Buildings of Irregular Cross-Sections Using Numerical Simulation. *Engineering Research Transcripts*, 7, 1–14.

DOI: https://doi.org/10.55084/grinrey/ERT/978-81-964105-4-4_1



1. Introduction

Wind is a very complex phenomenon, having infinite varieties of flow conditions. When it comes to the wind flow around a structure, it becomes very difficult to analyze the wind effects on it. So, it's very important to consider this part during the design stage of a structure for its safety and stability. It is to be noted that the wind condition during the design phase won't be the same once it starts functioning. The main reason for the variation in wind characteristics is the effect of surface friction. The objects on the ground surface causes an obstruction to the wind flow which causes it to slow down near the surface, whereas, an increase in height causes a decrease in the frictional effect which thereby increases the wind velocity. Hence, the wind action on tall building is to be given prior concern. The wind effect on tall buildings can also be related to the cantilever property of tall buildings which is fixed at ground level. The main points to be taken while considering wind are natural ventilation and structural stability. The pressure acting can be taken to determine the ventilation part, whereas forces can be considered for stability part. Interference effect in buildings should also be considered because the presence of adjacent structures influences the wind load acting on it. It will be entirely different from that of isolated conditions. The factors affecting the changes will be distance from adjacent structure, its shape, height, etc.

[1] calculated the uncertainties that arise while using computational fluid dynamics to forecast wind loads for full-scale constructions. [2] analyzed the properties of wind flow and the distribution of wind pressure on the surfaces of an octagonal-shaped building model. [3] studied the effects of wind on tall buildings using CFD simulation in various ways. [4] used CFD to analyze the interference effect of three identically tall square-plan buildings on the pressure at the faces of an octagonal-plan structure. [5] used CFD to conduct a numerical analysis of Y-shaped tall buildings. [6] conducted an experimental analysis on the various interference circumstances in building models with square and remodel-triangle shapes.

[7] weighed the benefits and drawbacks of choosing an atypical butterfly-shaped building over a square-shaped one. [8] studied the interference effect on a row of 3- square plan shaped buildings. [9] did a parametric study to determine the pressure distribution around a differential height structure. [10] looked at the wind-induced mean interference between L and T-shaped buildings that were placed close together. [11] presented information on ambient vibration collected during instances of strong winds to provide conclusions about the modal characteristics of two tall structures.

[12] examined the wind flow pattern and pressure distributions on the re-entrant wing facades of an irregular L-cross sectional form model at various wind incidence angles. [13] explored if a building model with an equal area and height and a regular or irregular cross-section would be affected by wind. The ratio of change in the cross-sectional form is maintained for both models with regular and irregular shapes. [14] found the pressure acting on each face of a Y-shaped tall building using both experimental and numerical methods. [15] determined the wind pressure on tall buildings with L and U shapes using both numerical and experimental research. [16] investigated behaviour of a pentagonal plan shaped building under varied wind incident angles.

This chapter deals with wind effect on fish-shaped high-rise buildings which is analyzed for isolated condition using Computational Fluid Dynamics in ANSYS CFX. The height of the building taken is of 60 m with a cross-sectional area of 400 m². The wind angle ranges from 0°-180° with a 15° interval.

2. Methodology

2.1. Turbulence Model

The model taken in this CFD study to simulate turbulence is k-ε model. In this model, the constantly changing components of turbulent velocity in all three directions are utilized to determine turbulent kinetic energy.

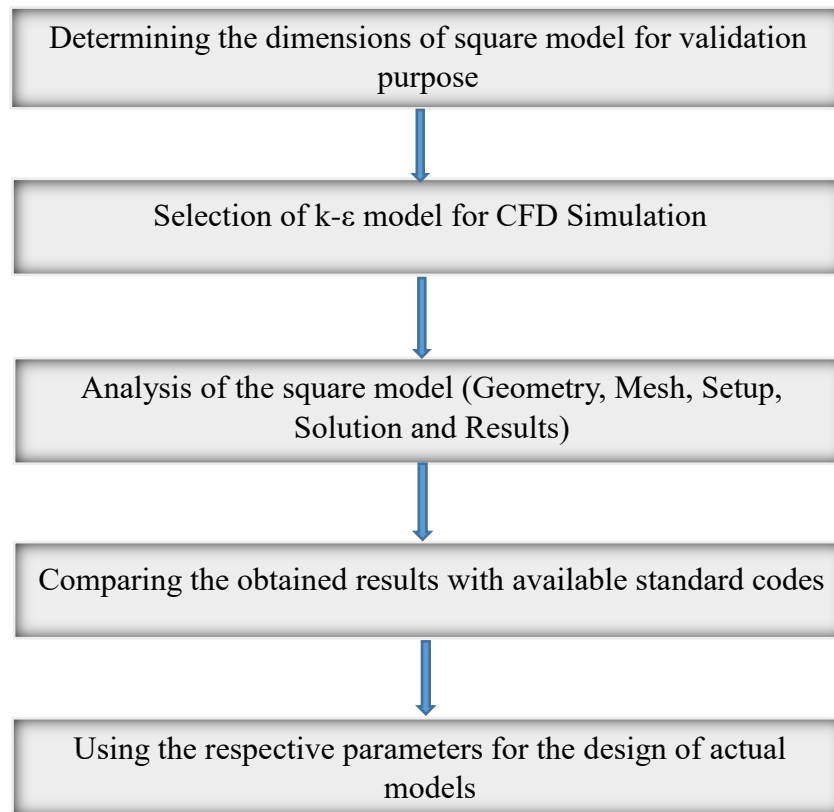


Fig. 1. Flowchart depicting the various steps to be followed in analysis

$$k = \frac{1}{2} \left(\overline{u^2} + \overline{v^2} + \overline{w^2} \right) \quad (1)$$

Here, k is the supplementary turbulent energy produced by the time-varying turbulent motions. From the turbulent kinetic energy, the calculation of turbulent dissipation ε is given as,

$$\varepsilon = \frac{k^{3/2}}{0.3D} \quad (2)$$

This equation is taken for the calculation of flows in pipe with a diameter D . And the closure equation is given as follows: For turbulent kinetic energy,

$$\rho \frac{\partial(u_i k)}{\partial x_i} = P_k + P_b - \rho \varepsilon + \frac{\partial}{\partial x_i} \left[\left(\mu + \frac{\mu_t}{\sigma_k} \right) \frac{\partial k}{\partial x_i} \right] \quad (3)$$

For turbulent dissipation,

$$\rho \frac{\partial(u_i \varepsilon)}{\partial x_i} = \frac{\partial}{\partial x_i} \left[\left(\mu + \frac{\mu_t}{\sigma_\varepsilon} \right) \frac{\partial \varepsilon}{\partial x_i} \right] + C_1 \frac{\varepsilon}{k} (P_k + C_3 P_b) - C_2 \rho \frac{\varepsilon^2}{k} \quad (4)$$

2.2. Validation

As a validation part of the study, the analysis is done on a square shaped tall building of height 60m and of the same cross-sectional area (400m^2). The obtained results are then compared with available standard codes, so as to determine its acceptability. These parameters are used for the analysis of Fish shaped building.

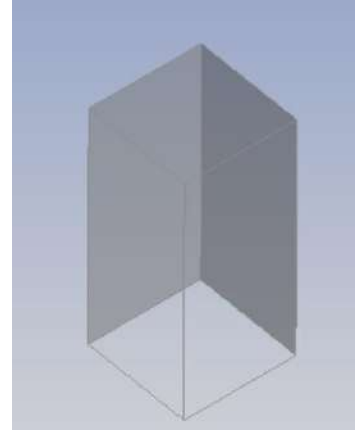
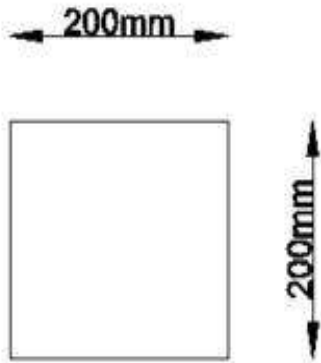


Fig. 2. Selected dimension of square model **Fig. 3.** Geometry of square model in ANSYS

The comparison of the obtained results with available code is given in the table below:

Table 1. Comparison of obtained result with IS:875 (Part III)- 2015

C_p at 0°	Faces of square model			
	A	B	C	D
IS:875 (Part III)-2015	+0.8	-0.25	-0.8	-0.8
Square Model	+0.75961	-0.27062	-0.73655	-0.73655

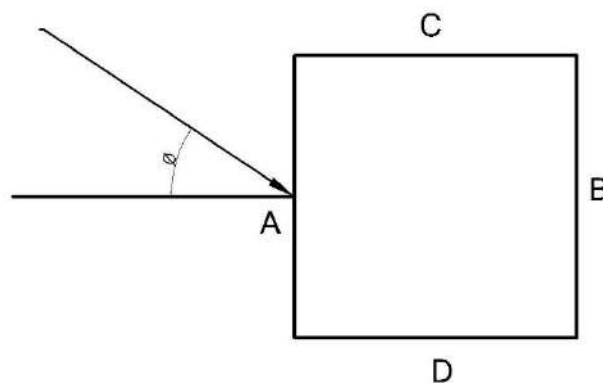


Fig. 4. Square model as per IS: 875 (Part III)- 2015

2.3. Numerical Analysis

Analysis using ANSYS involves five steps: geometry, meshing, setup, solution, and results. The model is imported from AutoCAD at the geometry stage. Once the building model is imported, the domain or the

wind tunnel is built around it according to international standards. The building is positioned inside the domain in such a way that the distance from windward face and lateral face is $5H$ and the distance from leeward face is taken as $15H$. The height of the domain from domain surface is taken as $6H$ (where, H is taken as the total height of the building). The wind incidence angle is also assigned in this step.

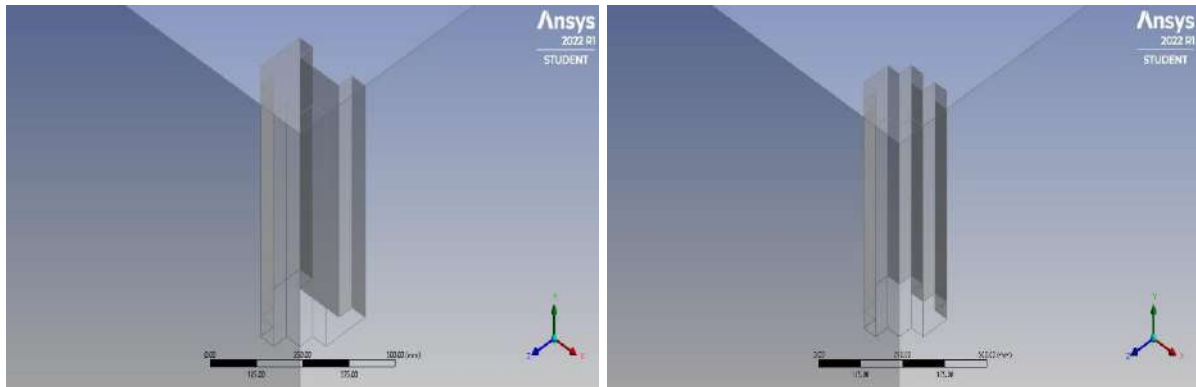


Fig. 5. Geometry of Model 1 and Model 2 in ANSYS

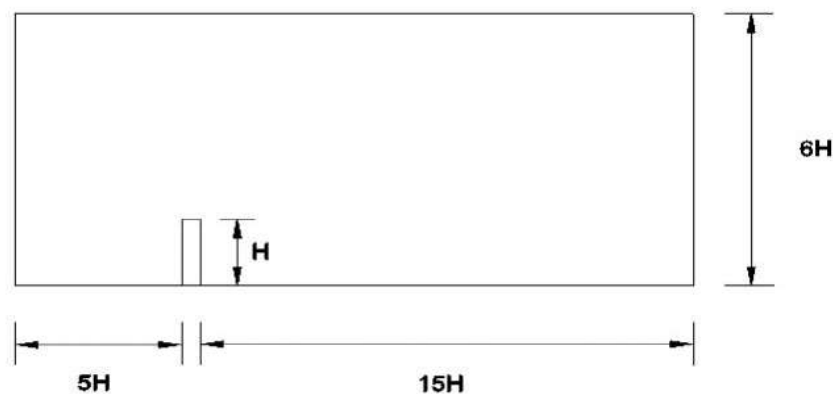


Fig. 6. Domain size

The prepared model is then taken to meshing stage where each face of the model is properly named. The meshing is provided as face mesh, edge mesh, ground mesh and inflation. The meshing size of the domain is taken as 0.2m.

The following boundary conditions are then assigned in the setup stage:

- Power-law is incorporated in the inlet.
- At the outlet 0 Pa is taken as the relative pressure.
- The side and top wall domain is taken as free slip wall, whereas the ground and building face is taken as no slip wall.

The power-law is considered here as the wind varies throughout the height of the building. The power-law is given by,

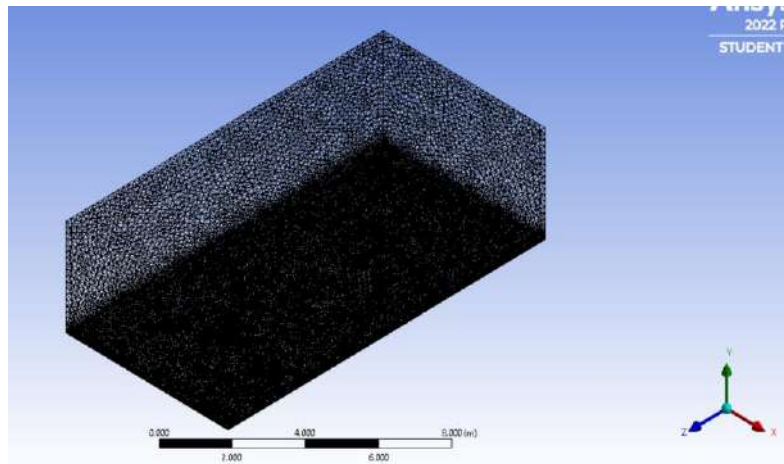
$$\frac{u}{u_{ref}} = \left(\frac{y}{y_{ref}} \right)^\alpha \quad (5)$$

where,

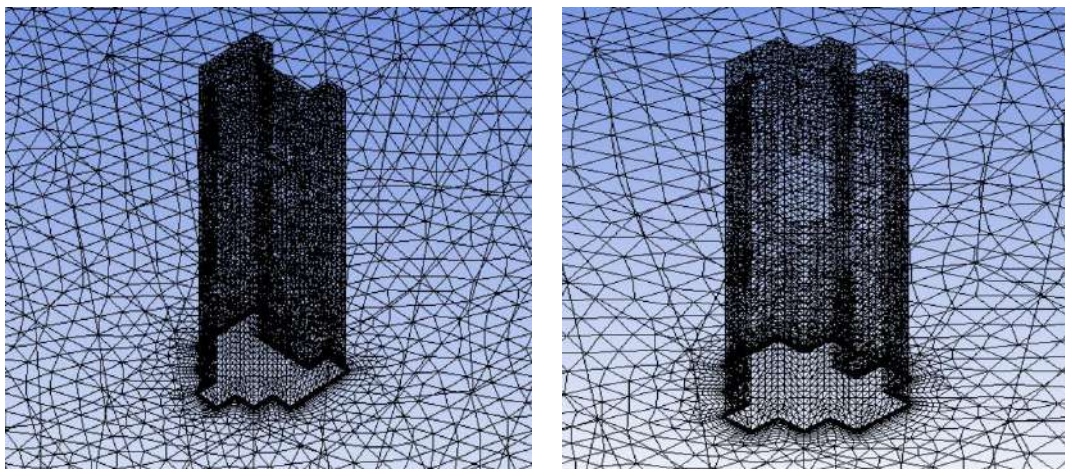
u_{ref} : reference velocity which is taken in accordance with the actual velocity. Here it's taken as 10 m/s

y_{ref} : reference height at which the velocity is known. The value taken is 1m

y : the height at which velocity is to be found out



(a)



(b)

Fig. 7. (a) Domain Meshing (b) Meshing of S-1 and S-2

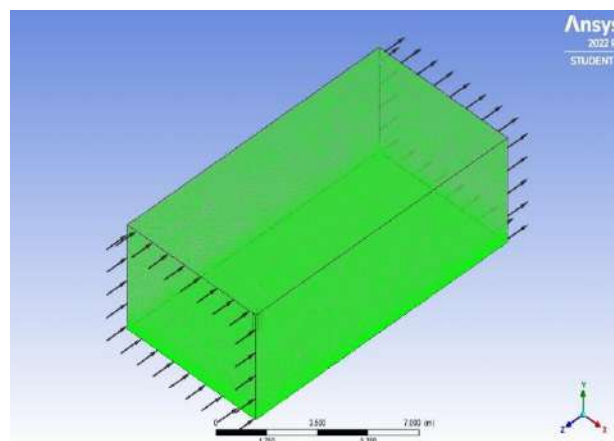


Fig. 8. Model after assigning boundary conditions

The model is run and the results are obtained. Lines are drawn on each face of the model to obtain pressure at each point. The value of pressure at each point on the lines are extracted to excel and the value of C_p is calculated as,

$$C_p = \frac{P}{0.5 \times \rho \times V^2} \quad (6)$$

where,

P : pressure

ρ : density of air (1.225kg/m^3)

V : wind velocity at known reference height

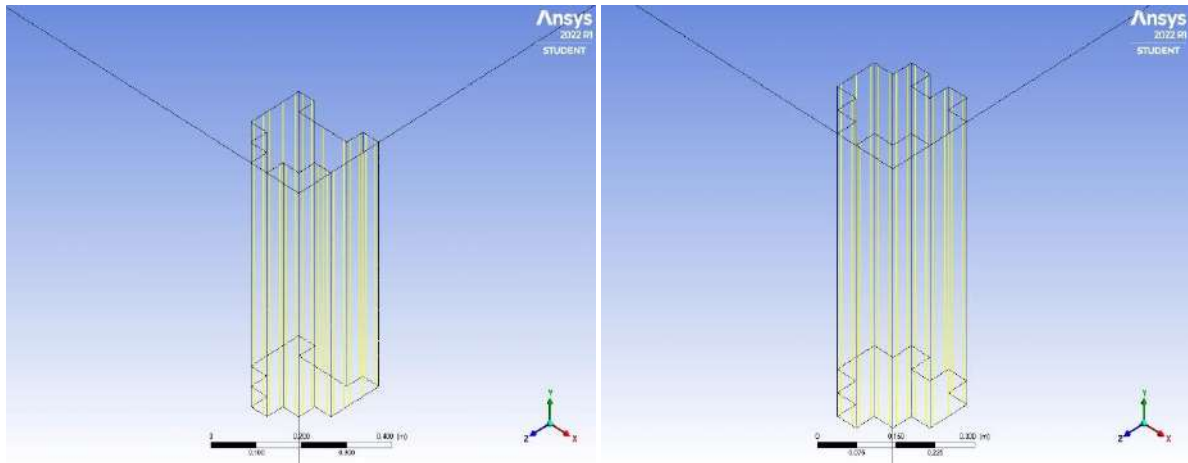


Fig. 9. Lines in post-CFX

3. Result and Discussions

The variation of coefficient of pressure with different wind incidence angle, the pressure contours of each face and the velocity streamlines are discussed here.

The face of the model is named as below:

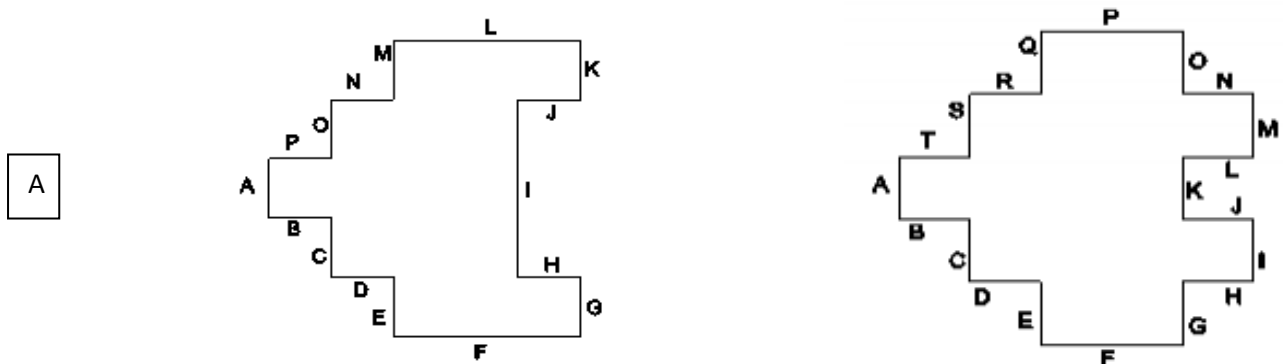
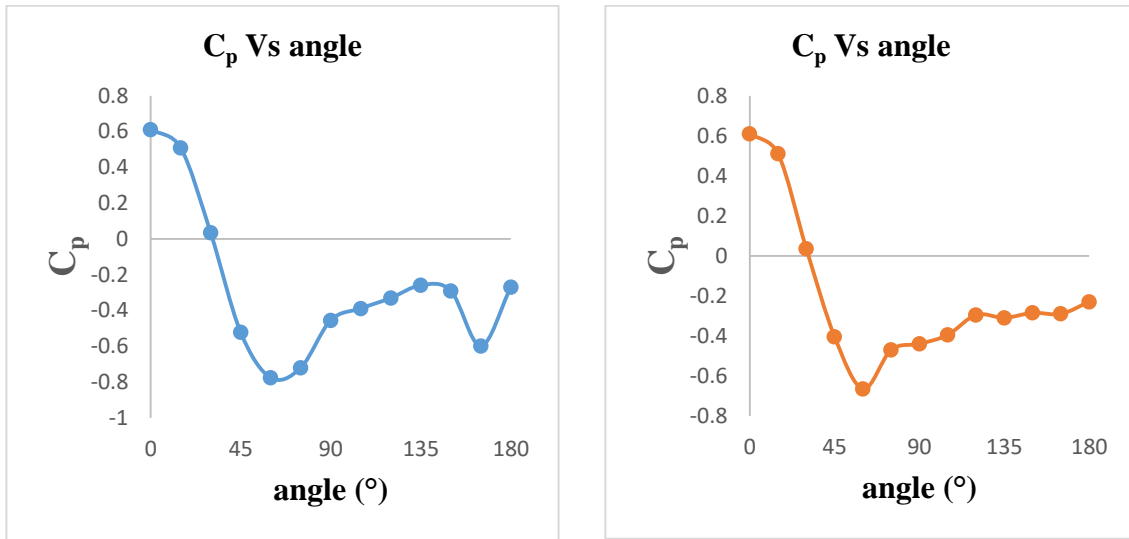


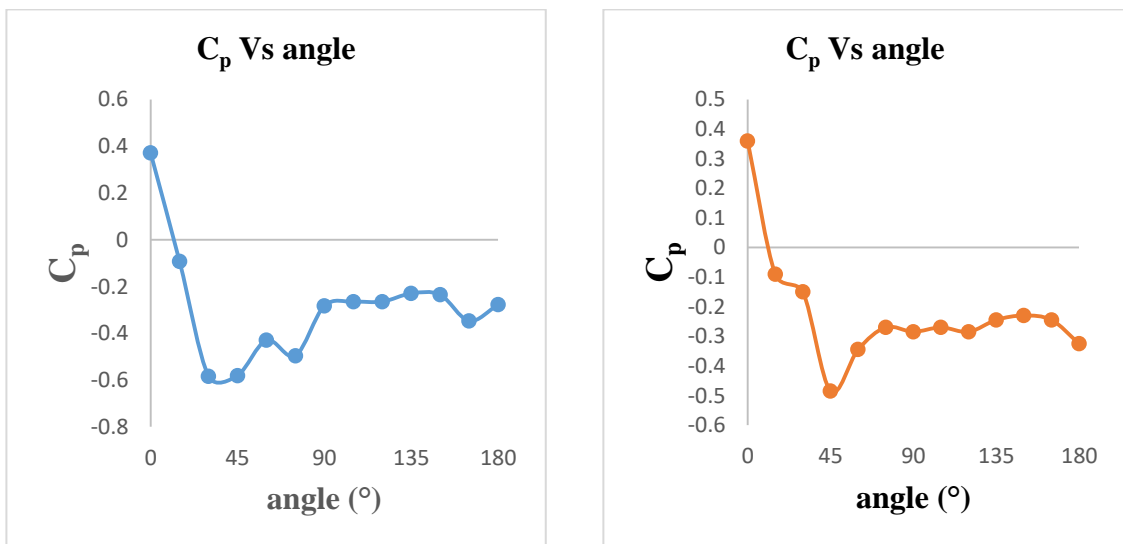
Fig. 10. Naming of model faces

3.1. Pressure coefficient

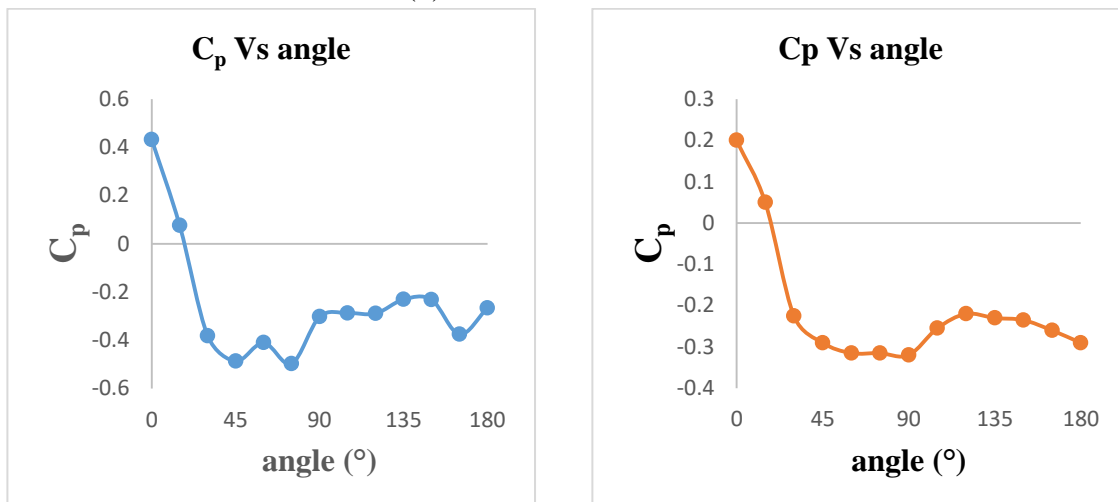
This factor is very important for a building to determine its air infiltration rate. The area of a surface, or its appropriate fraction, is multiplied by the pressure coefficient (C_p) and the design wind pressure at the surface's height above the ground to obtain the wind load operating normally on that surface, according to IS 875 (Part 3): 2015. The variation of coefficient of pressure with different wind incidence angle is represented in figure.



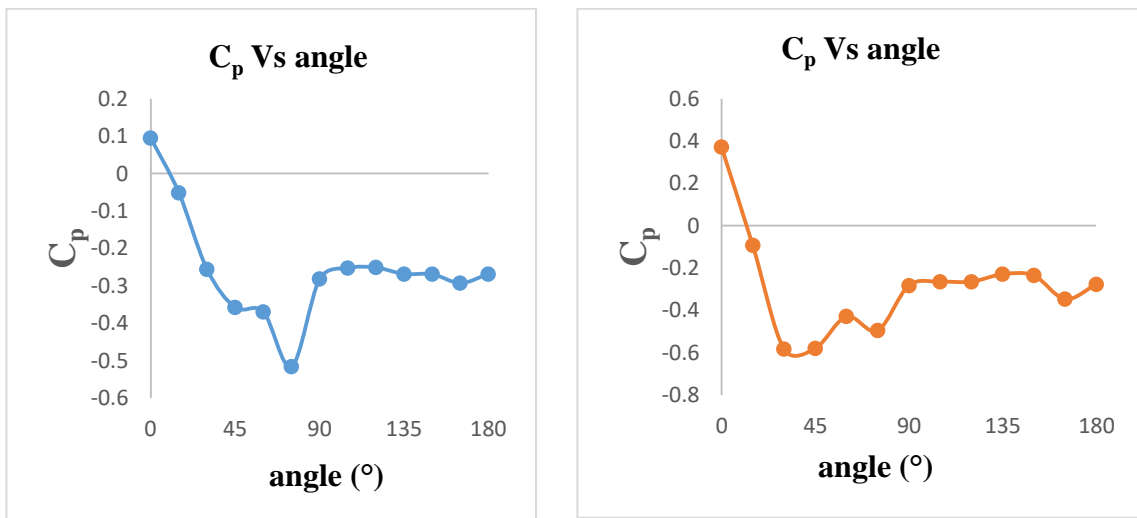
(a) Face A of S-1 and S-2



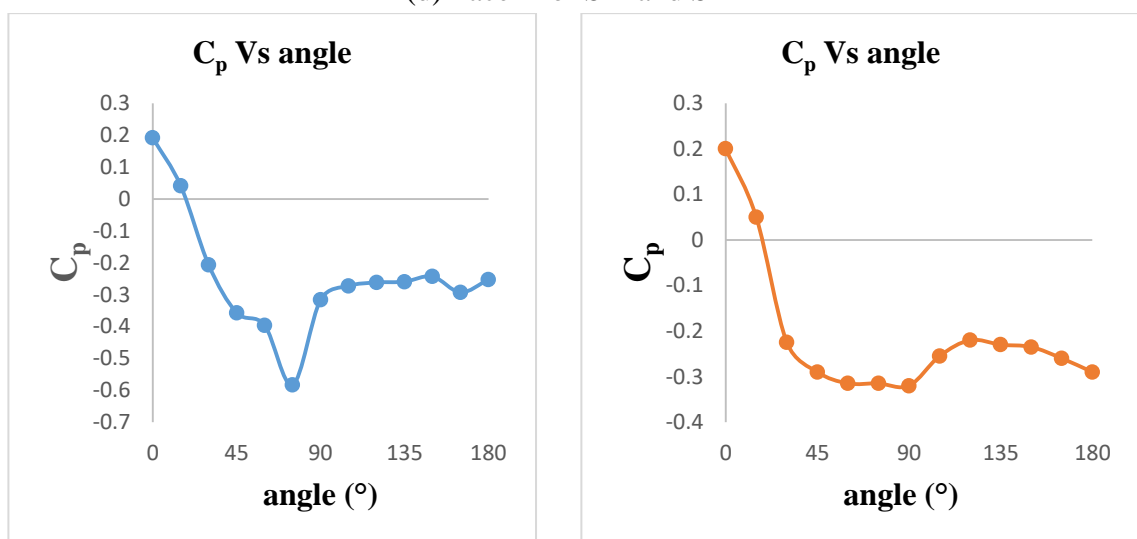
(b) Face B of S-1 and S-2



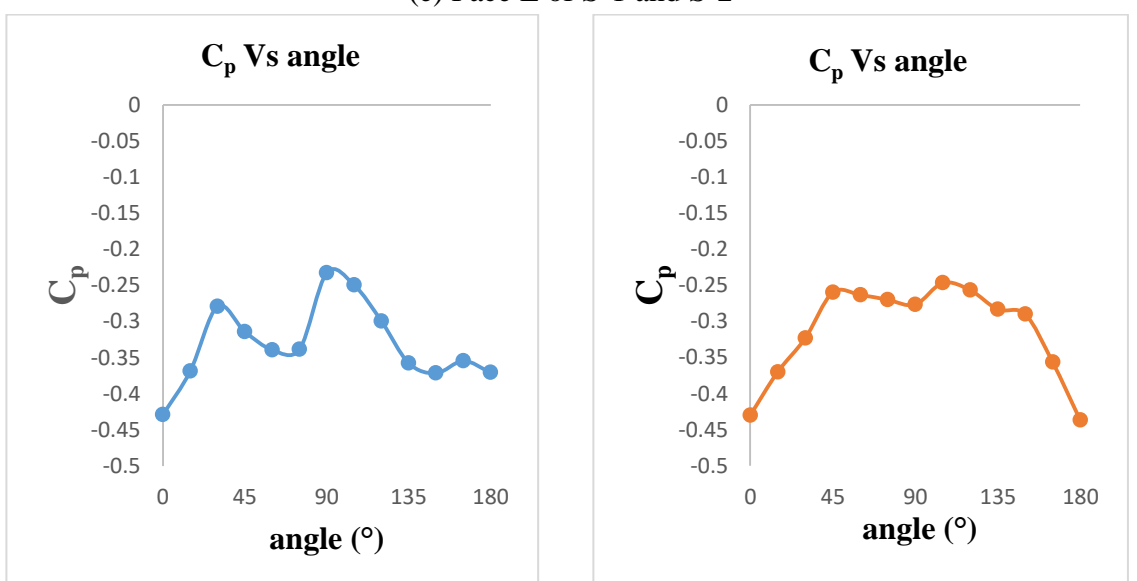
(c) Face C of S-1 and S-2



(d) Face D of S-1 and S-2



(e) Face E of S-1 and S-2



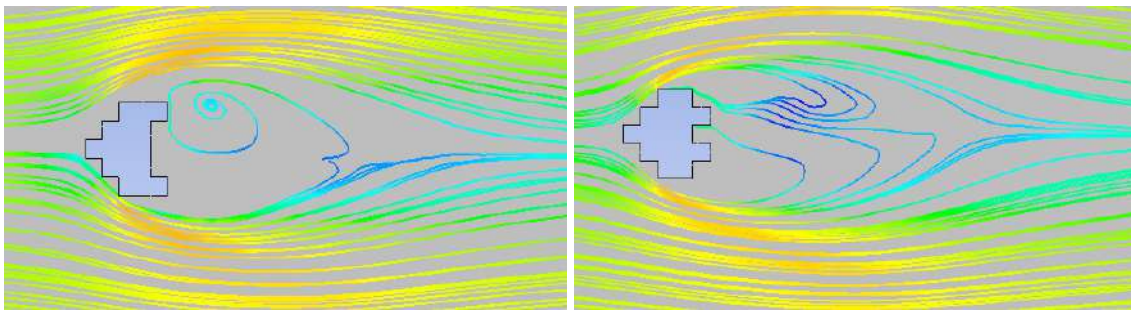
(f) Face F of S-1 and S-2

Fig. 11. Graphs showing variation of Cp for various faces

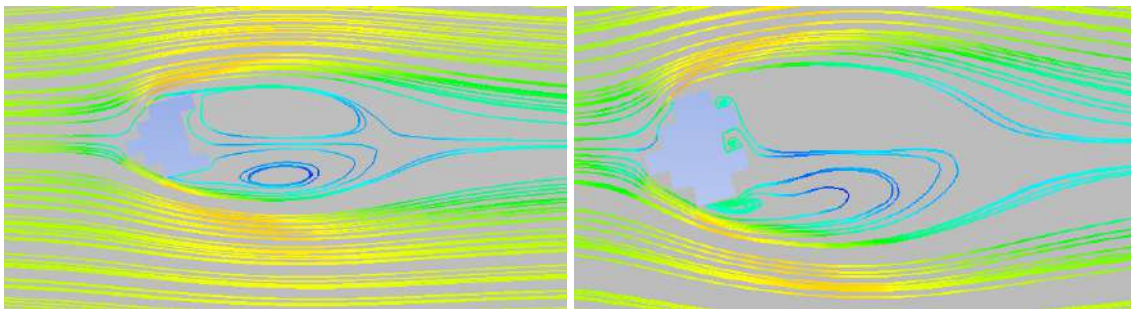
In Model 1, the maximum C_p value 0.65 is obtained in face I at a wind incidence angle of 180° and the minimum value -0.78 is observed on face A at an angle of 60° . Whereas in Model 2, the maximum value 0.65 is obtained on face N at 135° and minimum value -0.77 on face M at 105° . The variation in C_p is almost similar for faces A, B, C, D, E and F of both the models as shown in fig. There is a change from positive C_p to suction due to the formation of vortex. The change in other faces is due to the extra recession provided in model 2. Face F shows suction for every wind incidence angle in both the models. In model 2, face H also shows suction at every angles.

3.2. Velocity Streamlines

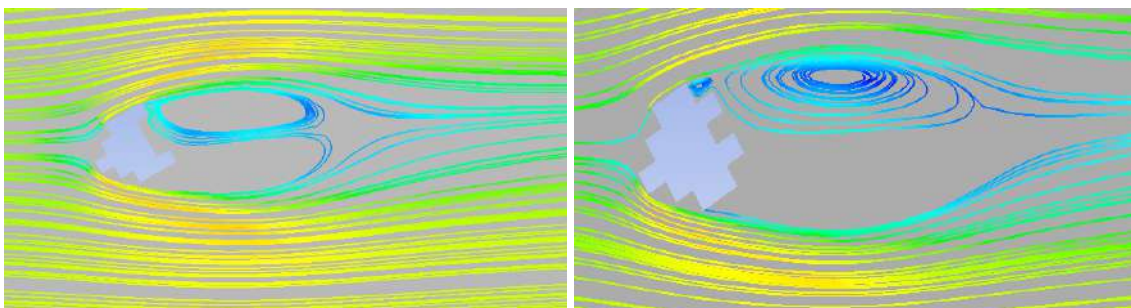
The tangent of velocity streamline at any point represents direction of velocity at that point. The velocity streamlines of model 1 and model 2 is taken at a height of 300mm from the ground surface, at all angles ranging from 0° to 180° at an interval of 15° . It is evident from the figures that the patterns are different for different angles as well as different for both the models. The colours in pattern represents the velocity, which is more on the windward side and decreases as it moves towards the leeward side. As the wind flow occurs across the building corners, recirculation and flow separation results in a decrease in flow velocity, as a result of which vortex is formed on the wake region. A suction zone is thus formed on the leeward side.



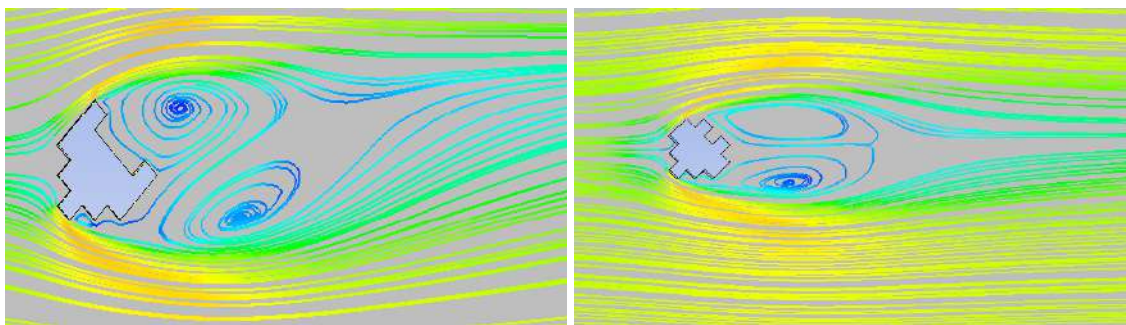
(a) Streamline patterns at 0° for S-1 and S-2



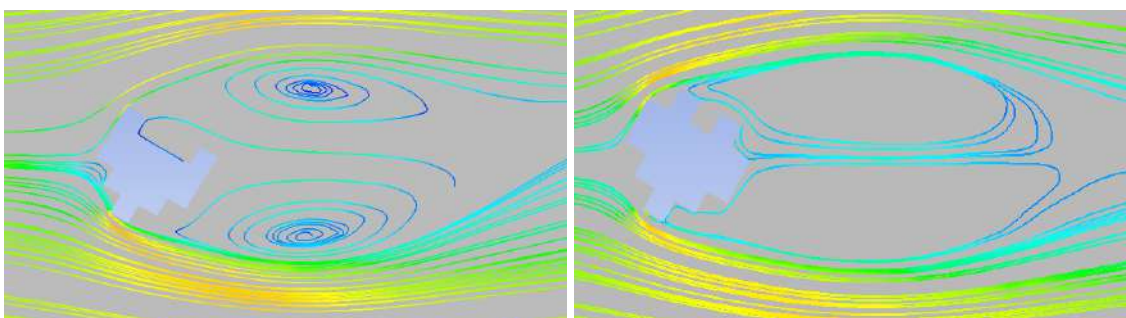
(b) Streamline patterns at 15° for S-1 and S-2



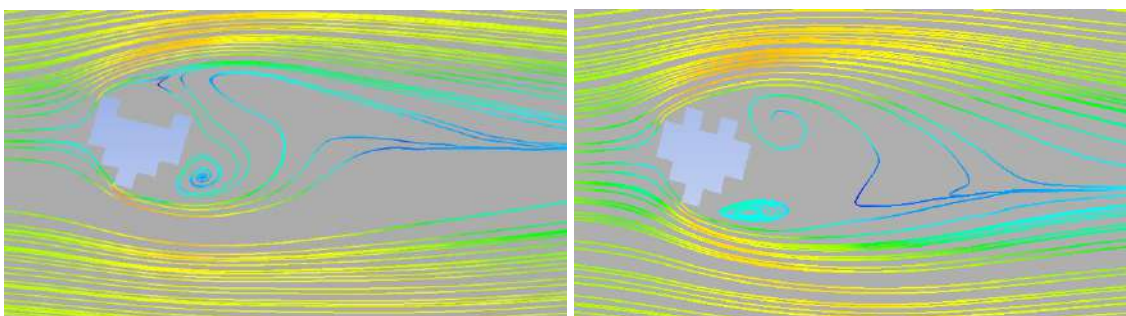
(c) Streamline patterns at 30° for S-1 and S-2



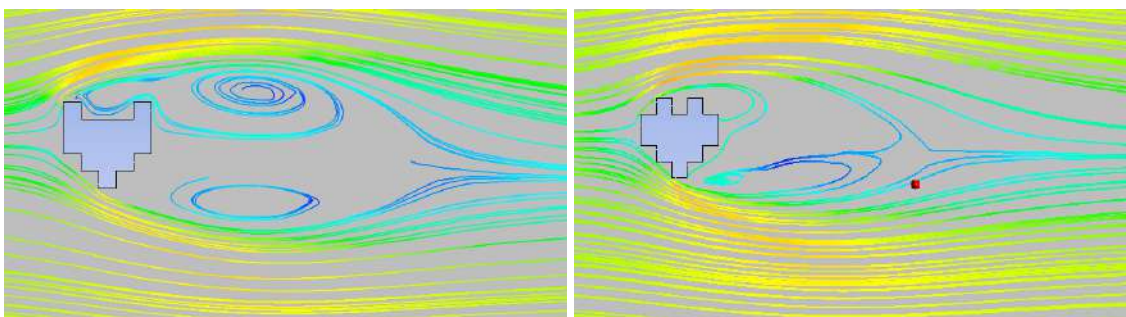
(d) Streamline patterns at 45° for S-1 and S-2



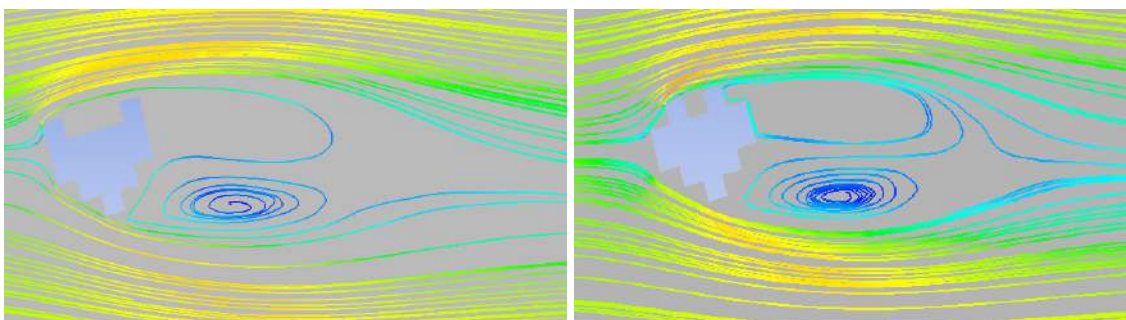
(e) Streamline patterns at 60° for S-1 and S-2



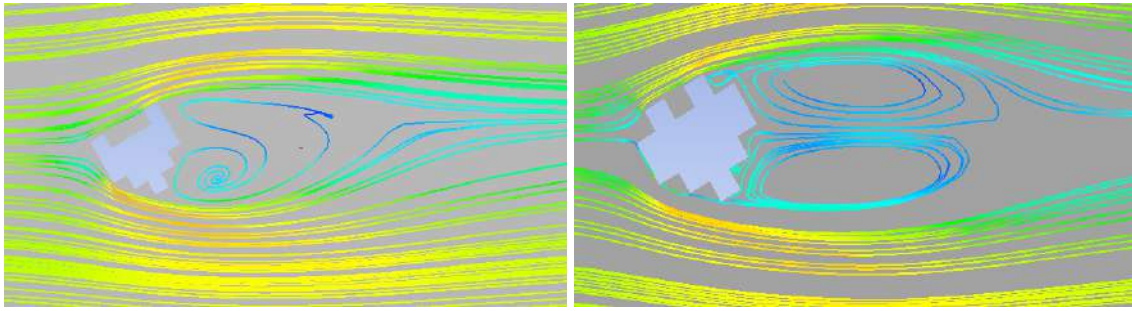
(f) Streamline patterns at 75° for S-1 and S-2



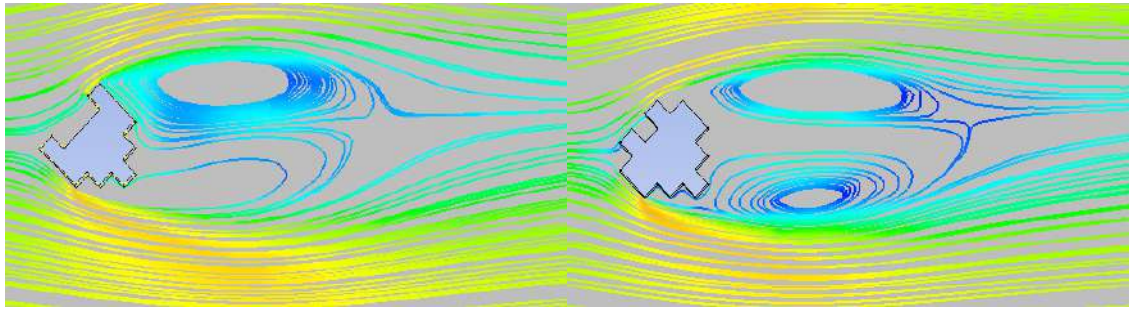
(g) Streamline patterns at 90° for S-1 and S-2



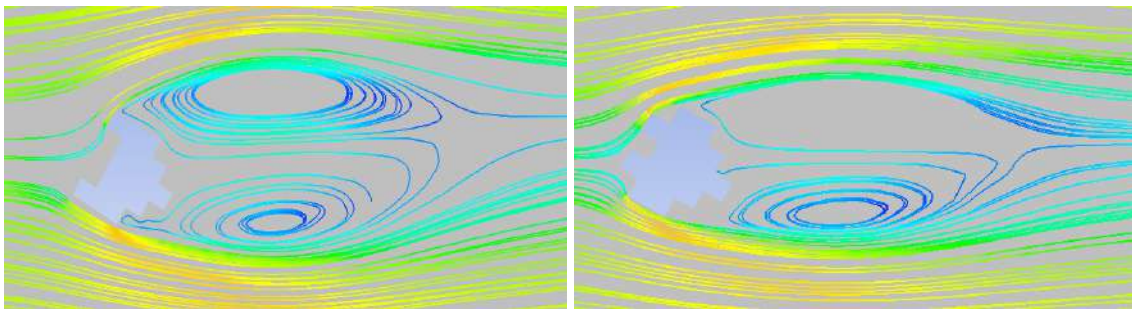
(h) Streamline patterns at 105° for S-1 and S-2



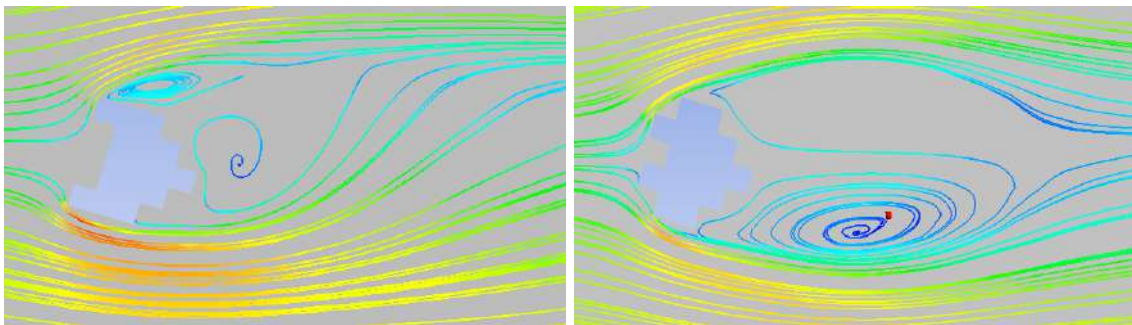
(i) Streamline patterns at 120° for S-1 and S-2



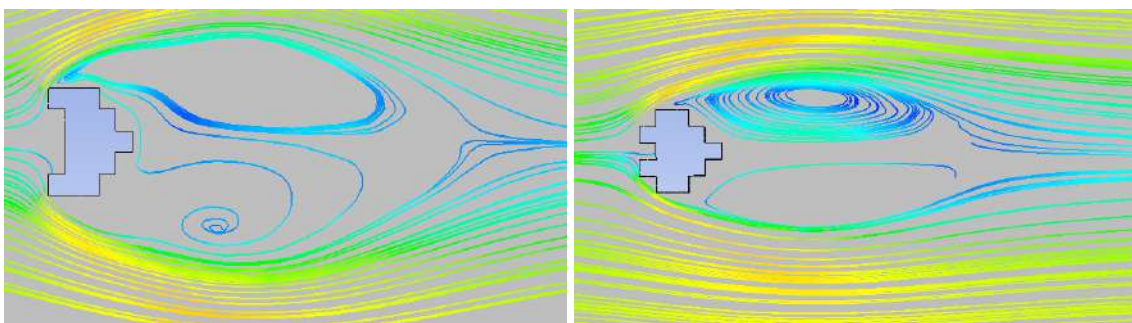
(j) Streamline patterns at 135° for S-1 and S-2



(k) Streamline patterns at 150° for S-1 and S-2



(l) Streamline patterns at 165° for S-1 and S-2



(m) Streamline patterns at 180° for S-1 and S-2

Fig. 12. Streamline patterns at various angles

Taking the case of both the models at 0° , we can see the vortex formation is not symmetrical. Its because of the turbulence which is caused during the flow. From examining the flow patterns, it can be seen that both the models perform well at 60° and almost symmetrical vortex is formed on both the side. The formation of symmetrical vortex shows that the building will be stable at that condition. It can be also seen that model 2 performs well in almost every wind angle and this can be related to its extra recessed corner.

4. Conclusions

The numerical simulation of Model 1 and Model 2 in isolated condition is done in this paper with the help of ANSYS CFX, at a scale of 1:100. The variation of C_p with wind incidence angle and the velocity streamlines of the models were analyzed and the following conclusions were drawn:

- The validation of the square model gives satisfactory results with respect to 1S:875 (Part III)- 2015.
- It is observed that C_p value is maximum when the wind direction is exactly perpendicular to the face and is minimum when it is inclined.
- The maximum C_p value observed was same for both model 1 and model 2.
- As both the models are similar in their front and side geometry, the variation of C_p with wind incidence angle is similar for some of the common faces.
- Streamlines are highly helpful for seeing the characteristics of flow separation and the creation of vortices in the wake zone. The combination of the pulling force on the leeward side and the positive force on the windward side produces vortices in the wake region, which deflects the body.
- When comparing the wind effect on simple and complex cross-sectional shaped tall buildings, the CFD methodology is more time and cost efficient than alternative approaches like wind tunnel testing.

References

- [1] Oliveira, P. J., & Younis, B. A. On the prediction of turbulent flows around full-scale buildings. *Journal of Wind Engineering and Industrial Aerodynamics*, 86(2–3), 203–220, 2000. [https://doi.org/10.1016/S0167-6105\(00\)00011-8](https://doi.org/10.1016/S0167-6105(00)00011-8)
- [2] A. Kumar and R. Raj, “Study of pressure distribution on an irregular octagonal plan oval-shape building using CFD,” *Civil Engineering Journal (Iran)*, vol. 7, no. 10, pp. 1787–1805, Oct. 2021, <https://doi.org/10.28991/cej-2021-03091760>.
- [3] R. K. Meena, R. Raj, and S. Anbukumar, “Wind Excited Action around Tall Building Having Different Corner Configurations,” *Advances in Civil Engineering*, vol. 2022, 2022, <https://doi.org/10.1155/2022/1529416>.
- [4] R. Kar and S. K. Dalui, “Wind interference effect on an octagonal plan shaped tall building due to square plan shaped tall buildings,” *International Journal of Advanced Structural Engineering*, vol. 8, no. 1, pp. 73–86, Mar. 2016, <https://doi.org/10.1007/s40091-016-0115-z>.
- [5] P. K. Goyal, S. Kumari, S. Singh, R. K. Saroj, R. K. Meena, and R. Raj, “Numerical Study of Wind Loads on Y Plan-Shaped Tall Building Using CFD,” *Civil Engineering Journal (Iran)*, vol. 8, no. 2, pp. 263–277, Feb. 2022, <https://doi.org/10.28991/CEJ-2022-08-02-06>.
- [6] R. K. Meena, R. R. Ahirwar, A. Srinivasan, R. Raj, and S. Anbukumar, *Analysis of Wind on Different Shape of High-Rise Structure*. International e-Conference on Sustainable Development & Recent Trends in Civil Engineering, 2022, Delhi, India
- [7] S. Bhattacharjee, S. Banerjee, S. G. Majumdar, A. Dey, and P. Sanyal, “Effects of Irregularity on a Butterfly Plan-Shaped Tall Building under Wind Load,” *Journal of The Institution of Engineers*

- (India): *Series A*, vol. 102, no. 2, pp. 451–467, Jun. 2021, <https://doi.org/10.1007/s40030-021-00511-6>.
- [8] K. Ming Lam, K. Lam, and J. Zhao, “Interference effects on wind loads on a row of tall buildings Investigation of heavy particles behavior in turbulence, The Fourth International Symposium on Computational Wind Engineering (CWE2006), Yokohama, 2006
- [9] R. G. Patel and S. D. Ramani, “Parametric Study to Understand Pressure Distribution Around Differential Height Structure.” *International Journal of Advance Research and Innovative Ideas in Education*, Vol-2 Issue-1 2016,
- [10] J. A. Amin and A. Ahuja, “Wind-induced mean interference effects between two closed spaced buildings,” *KSCE Journal of Civil Engineering*, vol. 16, no. 1, pp. 119–131, Jan. 2012, <https://doi.org/10.1007/s12205-012-1163-y>.
- [11] S. K. Au, F. L. Zhang, and P. To, “Field observations on modal properties of two tall buildings under strong wind,” *Journal of Wind Engineering and Industrial Aerodynamics*, vol. 101, pp. 12–23, 2012, <https://doi.org/10.1016/j.jweia.2011.12.002>.
- [12] A. Kumar and R. Raj, “CFD Study of Flow Characteristics and Pressure Distribution on Re-Entrant Wing Faces of L-Shape Buildings,” *Civil Engineering and Architecture*, vol. 10, no. 1, pp. 289–304, Jan. 2022, <https://doi.org/10.13189/cea.2022.100125>.
- [13] A. Verma, R. K. Meena, H. Dubey, R. Raj, and S. Anbukumar, “Wind Effects on Rectangular and Triaxial Symmetrical Tall Building Having Equal Area and Height,” *Complexity*, vol. 2022, 2022, <https://doi.org/10.1155/2022/4815623>.
- [14] S. Mukherjee, S. Chakraborty, S. K. Daluf, and A. K. Ahuja, “Wind induced pressure on ‘Y’ plan shape tall building,” *Wind and Structures, An International Journal*, vol. 19, no. 5, pp. 523–540, Nov. 2014, <https://doi.org/10.12989/was.2014.19.5.523>.
- [15] M. G. Gomes, A. Moret Rodrigues, and P. Mendes, “Experimental and numerical study of wind pressures on irregular-plan shapes,” *Journal of Wind Engineering and Industrial Aerodynamics*, vol. 93, no. 10, pp. 741–756, 2005, <https://doi.org/10.1016/j.jweia.2005.08.008>.
- [16] L. Sobankumar, S. Prabavathy, and R. Vigneshwaran, “Study on wind flow around a pentagon plan shape tall building using CFD,” in *Journal of Physics: Conference Series*, Jul. 2021, vol. 1850, no. 1. <https://doi.org/10.1088/1742-6596/1850/1/012045>.